의학석사 학위논문

Activity-dependent metaplasticity of direct cortical inputs in the rat hippocampal CA3 pyramidal neuron

백서 해마에서의 CA3 영역 추체세포 자극에 의한 신경가소성의 변조 현상에 대한 연구

2014년 02월

서울대학교 대학원

의과학과

엄 기 상

백서 해마에서의 CA3 영역 추체세포 자극에 의한 신경가소성의 변조 현상에 대한 연구

지도교수 이 석 호

이 논문을 의학석사 학위논문으로 제출함

2013년 10월

서울대학교 대학원

의과학과

엄 기 상

엄기상의 의학석사 학위논문을 인준함

2014년 1월

위 원 장 _____ (인)

부위원장 _____ (인)

위 원 _____ (인)

Activity-dependent metaplasticity of direct cortical inputs in the rat hippocampal CA3 pyramidal neuron

by

Kisang Eom

A thesis submitted to the Department of Biomedical Sciences in partial fulfillment of the requirements for the Degree of Master of Science in Medicine at Seoul National University College of Medicine

October 2013

Approved by Thesis Committee:

Professor _____Chairman

Professor _____Vice chairman

Professor _____

ABSTRACT

The intrinsic excitability of neurons plays an important role in the encoding of memory and in the coupling of synaptic inputs to spike generation. Recently, we report that repetitive somatic firing with physiologically relevant frequency induces internalization of Kv1.2 from distal dendrites of hippocampal CA3 pyramidal cells (CA3-PCs), resulting in long-term potentiation of intrinsic excitability (LTP-IE). We posed a question whether LTP-IE has any differential influences on the synaptic modulation at distal and intermediate dendritic intputs, which are carried by perforant path (PP) and associational/commissural (A/C) fiber, respectively.

I monitored the excitatory postsynaptic potentials (EPSPs) every 8 s at PP-CA3 synapses and AC-CA3 synapses before and after 'conditioning' (a train of 20 somatic action potentials at 10 Hz) in CA3 PC. This conditioning induced a potentiation of EPSPs but not EPSCs at PP-CA3 synapses, whereas the same priming signal altered neither EPSCs nor EPSPs at AC-CA3 synapses.

To study the effect of LTP-IE on metaplsticity at PP-CA3 synapses, I first determined the threshold in the strength of PP stimulation for induction of long-term potentiation (LTP) at PP-CA3 synapses. I found that minimal stimulation of PP-CA3 synapses at high frequency (weak HFS) by itself was below the threshold of LTP induction. The weak HFS of PP induced neither EPSP-to-spike (E-S) potentiation nor LTP under control conditions. After the

induction of LTP-IE, however, weak HFS readily induced E-S potentiation and LTP at the PP-CA3 synapses.

These results indicate that LTP-IE in the CA3-PCs enhances E-S coupling specifically at the PP synapses, which in turn facilitates memory formation at the same synapse under Hebbian rule.

Keywords: hippocampus, metaplasticity, long-term potentiation, intrinsic plasticity

Student Number: 2012-21801

LIST OF FIGURES

CONTENTS

INTRODUCTION

1. CA3 of Hippocampus: Pathways and Functions

The connus area of hippocampus proper (CA3) plays a role in rapid encoding of new contexts, spatial working memory, pattern separation, and pattern completion (Leutgeb and Leutgeb, 2007; Nakazawa et al, 2002; Kesner, 2007). CA3 pyramidal cells (CA3-PC) receive external excitatory inputs directly and indirectly from entorhinal cortex (EC) and auto-associational input termed associational/commissural input (A/C) (Baker et al, 2011; Steward, 1976; Witter and Amaral, 1991). The indirect input from EC layer II is conveyed through axon fibers of dentate granule cells, so-called mossy fibers (MFs), disynaptically (Steward, 1976; Witter and Amaral, 1991). The MFs innervate proximal apical dendrites of CA3-PCs via specialized synaptic structures, thorny excrescence, in the striatum lucidum (Claiborne et al. 1986). Inspired by such a large structure of MF synapses onto CA3-PCs, McNaughton et al. (McNaughton and Morris, 1987) proposed that the MF input to CA3 may play an instructing role in encoding of memory at direct cortical synapses.

Another important external input is conveyed monosynaptically from stellate cells EC layer II via perforant pathway (PP, axons of stellate cell in EC layer II). PP inputs are comprised of medial and lateral components (Stafekhina and Vinogradova, 1978). It has been suggested that the former transmits spatial information, whereas the latter non-spatial information (e.g. olfactory, auditory information). In Long-Evans rats, lesion of medial EC impairs

(Ferbinteanu et al. 1999). Hunsaker et al. (Hunsaker et al. 2007) showed that infusion of AP-5 or naloxone into CA3a,b disrupted both novelty detection of spatial location and a visual input, whereas naloxone into CA1 disrupted only novelty detection of visual input.

Recurrent excitatory connections between CA3-PCs via associational/commissural (A/C) fibers constitute the auto-associational network in CA3 (Steward, 1976; Witter and Amaral, 1991). A/C fibres make synaptic contact on dendrites of CA3-PCs in striatum radiatum (Steward, 1976; Witter and Amaral, 1991; Ishizuka et al, 1990). This extensive network of recurrent collaterals led to a hypothesis that the CA3 associative network is capable to retrieve entire memory patterns from partial or degraded inputs, so-called pattern completion (McNaughton and Morris, 1987; Hasselmo et al, 1995; Vazdarjanova and Guzowski, 2004). In CA3, the synaptic strength of recurrent synapses along with perforant path synapse can be modified by NMDA receptor (Stoop et al, 2003). And NMDA receptors of CA3-PC are required for the associative memory recall (Nakazawa et al, 2002).

In summary, it has been proposed that MF synaptic inputs govern encoding of new memory at PP synapses on CA3-PCs, whereas recurrent synapses encode memory necessary for retrieval of entire pattern from partial cues. Moreover, PP synaptic inputs convey spatial or non-spatial sensory information, and initiates retrieval from CA3 autoassociaton network. This theory of hippocampus proposes an associative Hebbian synaptic modification at PP synapses in a CA3-PC detonated by a strong MF input as a biological

mechanism for the instructing role of MF inputs. Consistently, associative LTP of EPSPs at PP synapses (PP-EPSPs) could be induced by simultaneous high-frequency stimulation (HFS) of PP and MFs (McMahon and Barioneuvo, 2001). It has been shown that heterosynaptic potentiation of PP-EPSPs can be induced by HFS of MF alone (Tsukamoto et al, 2003), but this finding was not presumed by the hippocampal theory, raising a possibility that MF inputs may have influences on the CA3 network by a mechanism different from the prediction of the hippocampal theory (McNaughton and Morris, 1987).

2. Long-term potentiation of intrinsic excitability (LTP-IE)

Although synaptic plasticity is considered cellular mechanism of information processing, it is not an exclusive mechanism (Daoudal and Debanne 2003; Campanac and Debanne 2007). Persistent regulations of ionic conductance in certain areas of neuron, such as dendrites and soma, also may have a role for information processing (Sehgal et al, 2013). Investigations about long-term activity-dependent alternations of properties of ionic conductance have been reported previously. Stimulation of hippocampal CA1 pyramidal neuron with synaptic inputs correlating with postsynaptic neuronal spikes elicits synaptic LTP and LTP-IE mediated by A-type K^+ currents (Xu et al, 2005). And downregulation of A-type K^+ current after synaptic LTP is mediated by calcium/calmodulin-dependent protein kinase II and clathrin-mediated endocytosis (Jung et al, 2006).

The change of ionic conductance by K^+-current after conditioning activities

without synaptic plasticity was reported previously. For basket cells in hippocampal CA1 region, LTP-IE is induced by metabotropic glutamate receptor type 5 (mGluR5) and mediated downregulation of D-type K^+ current subunit Kv1.1 (Campagnac et al, 2013). For CA3-PCs, D-type K^+ current subunit kv1.2 was downregulated and neuronal excitability was increased after conditioning by repetitive somatic firing at 10 Hz for 2 s (Hyun et al, 2013). This finding raises a possibility that the somatic firing-induced the increase in excitability may underlie the MF-induced heterosynaptic potentiation of PP inputs that has been reported (Tsukamoto et al, 2003). Therefore, I posed the question whether the excitability change induced by such conditioning can modulate the threshold of LTP at PP-CA3 or A/C-CA3 synapses.

3. Metaplasticity

Metaplasticity is a change in a threshold for synaptic plasticity caused by a neural activity preceding the synaptic plasticity-inducing event (Abraham and Bear, 1996). There are many evidences about long-term potentiation (LTP) or long-term depression (LTD) as a molecular mechanism for encoding of memory (Martin et al, 2000). However, mechanisms for maintaining balance between LTP and LTD are also necessary to prevent saturation of LTP or LTD that could compromise the ability of networks to discriminate events or store information (Moser et al, 1998). There are various neuromodulators that regulate degrees of LTP or LTD in conjunction with plasticity-inducing events

(Lynch et al, 1988; Thiels et al, 1994). However, different kind of mechanisms to regulate synaptic plasticity also exists. A neural activity called 'priming signal' at one point of time can regulate synaptic plasticity that is induced by subsequent plasticity-inducing events (Abraham and Bear, 1996). This regulation of synaptic plasticity by preceding neural activity is termed 'metaplasticity'. The priming signal can comprise electrical stimulation of neural activity, pharmacological stimulation of neurotransmitter (Abraham. 2008). In metaplasticity, physiological or biochemical changes induced by bout of neural activity persists after termination or washout of priming signal and synaptic plasticity is induced by subsequent plasticity-inducing signal. That is important difference from conventional plasticity modulation, which is modulation occurs in conjunction with induction of synaptic plasticity. Several mechanisms of metaplasticity were reported. In area CA1 of hippocampus, prior activation of NMDA receptors inhibits LTP induction (Huang et al, 1992). And NMDA receptor activation by priming stimulation can also facilitate LTD without itself causing persistent synaptic plasticity (Mockett et al, 2002).

Metabotropic glutamate receptors (mGluRs) also modulate synaptic plasticity. Activation of group 1 metabotropic glutamate receptors (mGluR1) facilitates both the induction and the persistence of subsequent LTP in the area CA1 (Cohen et al, 1999). In this investigation, increased induction of LTP in CA1 is mediated by long-term downregulation of Ca^{2+}-activated K^{+} current that underlies the slow after-hyperpolaization (slow AHP).

Activity of one synapse can affect subsequent change of not only itself, but also neighbouring synapses (Abraham et al, 2001). Holland et al. (1998) represented strong priming stimulation induced facilitation of LTD and inhibition of LTP induction in neighbouring synapses. Hunt et al. (2013) reported that heterosynaptic metaplasticity between MF and A/C in was mediated by NMDA receptor LTP of MF.

Because both LTP and LTD are depolarization-dependent process, metaplasticity might arise from the changes of membrane property of postsynaptic neuron. Both A-type K^+ channel and hyperpolariziation-activated cation channel (I_h) showed long-term reductions of these channels after priming stimulation and regulation of LTP and LTD after the reduction of these channels (Ramakers and Storm, 2002; Brager and Johnston, 2007). However, in CA3 region of hippocampus, metaplasticity of perforant path have not been studied intensively. I show here that repetitive somatic current injection induces potentiation of EPSPs and EPSP-to-spike (E-S) coupling only at PP-CA3 synapse, and that such E-S potentiation in turn lower the threshold for LTP induction at the same synapse.

MATERIALS AND METHODS

1. Slice Preparation

Hippocampal brain slice was obtained from Sprague-Dawley rats (Postnatal days 15~19) of either sex as described previously (Lee et al, 2007). Protocols were approved by the Animal Care Committee of Seoul National University. Rats were anaesthetized with isoflurane and decapitated, and brain was quickly removed and chilled with high-magnesium preparation solution containing (in mM): 116 NaCl, 26 $NaHCO_3$, 3.2 KCl, 0.5 $CaCl_2$, 7 $MgCl_2$, 1.25 NaH_2PO_4, 10 glucose, 2 sodium pyruvate, 3 ascorbate, with pH 7.4 adjusted by saturating with carbogen (95% O2, 5% CO2). The isolated brain was mounted onto the stage of a vibratome (Leica VT1200) and acute transverse hippocampal slices were sectioned with 300 μm-thickness. After slices were made, a deep cut was made along hippocampal sulcus and across the edge of dentate molecular layer and hilus using a curved scalpel to cut entorhino-dentate connections and mossy fiber to prevent contamination of synaptic inputs from dentate gyrus with monosynaptic or polysynaptic components via the two connections described above. After cut, the slices were incubated at 34-36 ℃ for 30 min, and thereafter maintained at room temperature until required in same solution. For experiments, slices were transferred to a recording chamber superfused with artificial cerebrospinal fluid (aCSF) containing: (124 NaCl, 26 $NaHCO_3$, 3.2 KCl, 2.5 $CaCl_2$, 1.3 $MgCl_2$, 1.25 NaH_2PO_4, 10 glucose, pH was adjusted by saturating with 95% O2 and 5% CO2).

2. Electrophysiological Experiments

All recordings were performed in aCSF containing $GABA_A$ receptor antagonists (100 μM picrotoxin). Whole-cell voltage- or current-clamp recordings from hippocampal CA3-PCs (one cell per slice) were carried out 30 - 34℃ while the chamber was superfused with aCSF with 1 - 1.5 ml min^{-1}. EPSCs or EPSPs were evoked using an extracellular stimulating electrode (concentric bipolar CBAPB125, FHC, Inc., ME, USA). Brief (100 μs stimulation) pulses were delivered with intensities of 1 - 9 V and 1 - 8 V to the PP pathway and A/C fibers, respectively. PP responses were evoked by a bipolar electrode placed in stratum laculosum-moleculare. Distal A/C and proximal A/C responses were evoked by stimulation in distal (250-300 μm) and proximal (150-200 μm) location of striatum radiatum of CA3, respectively. Recordings were performed with a Multiclamp 700B Amplifier controlled by Clampex 10.2 through a Digidata 1440A data acquisition system (Molecular Devices, Sunnyvale, CA, USA) with a pipette solution containing (in mM): 130 potassium gluconate, 7 KCl, 2 NaCl, 1 $MgCl_2$, 0.1 EGTA, 2 ATP-Mg, 0.3 Na-GTP, 10 Hepes (pH 7.30 with KOH, 295 mosmol l-1 with sucrose). After whole-cell configuration on a soma of CA3-PC were formed, only cells that had stable resting membrane potential within -76 and -58 mV (cells that had more positive resting membrane potential or unstable resting membrane potential was discarded). After cells were stabilized, EPSPs or EPSCs were continuously monitored by delivering brief stimuli with extracellular stimulating electrodes every 8 s or 10 s, respectively.

3. Minimal stimulation techniques

In some experiments for PP-CA3 synapses, EPSCs and EPSPs were evoked by minimal stimulation. The techniques as described previously (Dobrunz et al, 1997; Perez-Rosello et al. 2002; Raastad, 1995). The stimulation intensity was gradually increased until EPSC can be evoked in an all-or-none manner depending on the stimulation intensity. Just above the threshold, I could find a range of stimulus intensity such that EPSCs/EPSPs were evoked with a failure rate of 40-60 % and that the average amplitude of EPSCs/EPSPs were relatively stationary (refer figure 2C).

4. Data Analysis

Data were acquired and digitized with an analogue-to-digital converter (Digidata 1440A, Molecular Devices) and stored in a computer hard disk. Analysis of data was performed IgorPro (version 6.10A; WaveMetrics, Lake Oswego, OR, USA) and Clampfit 10.2 (Molecular Devices, Sunnyvale, CA, USA). Statistical data are expressed as mean ± standard error of the mean (SEM) and *n* indicates the number of cells studied. Statistical analysis was performed using Wilcoxon signed rank test and Friedman test with PASW, version 18 (*SPSS* Inc., Chicago, IL, USA) for 2-paired data and 3-paired data, respectively. For non-paired data, Mann-Whitney *U* test was performed. A *p*-value of 0.05 was considered as statistically significant.

RESULTS

1. Conditioning of the CA3 pyramidal neurons with repetitive somatic firing induces potentiation of EPSP at PP-CA3 synapses, but not at A/C-CA3 synapses

Once whole-cell configuration of CA3-PC was formed, membrane potential was adjusted -70 ± 2 mV and -60 mV in current-clamp mode and voltage-clamp, respectively. Test pulses were delivered to evoke EPSPs and EPSCs every 8 s and 10 s, respectively. After stable baseline EPSPs were obtained, short trains of suprathreshold somatic current injection (1200 pA, 2.2 ms pulses) was applied for 2 s at 10 Hz to evoke somatic firing (inset of Figure 1A). Hereafter this repetitive somatic current injection is to be termed 'conditioning'. EPSPs evoked by stimulation of PP (PP-EPSPs) or EPSPs by stimulation of A/C fibers (A/C-EPSPs) were monitored every 8 s, and normalized with the average amplitude of baseline EPSPs measured before the conditioning. Time points of the conditioning are indicated with blue arrowheads in Figure 1A. After 30 min from the conditioning, bath application of DCG-IV (2 μM) to discriminate PP inputs and A/C inputs. EPSCs were assessed before the start of EPSP monitoring and after 20 min after the conditioning. Figure 1A shows relative changes of EPSPs as a function of time elapsed after the conditioning. Only PP-EPSPs (Figure 1A1) were potentiated, but EPSPs at A/C synapses on the distal axial dendrites (distal AC-EPSPs, 200 - 300 μm from the soma, Figure 1A2) and those on

proximal axial dendrites (proximal AC-EPSPs, 150 - 200 μm from the soma, Figure 1A3) were not. The PP-EPSP amplitudes were attenuated by bath application of DCG-IV by 75%. Figure 1B1-1B3 summarizes the averaged amplitude of EPSPs before and after the conditioning at PP-CA3, distal A/C-CA3, and proximal A/C-CA3 respectively. Only PP-EPSPs were significantly potentiated after the conditioning (175.03 ± 38.32%, $p = 0.028$, $n = 6$). EPSPs of distal AC-EPSPs (101.73 ± 13.65%, $n = 6$, $p = 0.917$) and proximal AC-EPSPs (96.79 ± 16.31%, $n = 3$, $p = 0.593$) were not affected by the same conditioning. Figure 1C1-1C3 show that the averaged amplitude of EPSCs was not altered after the conditioning at PP-CA3 synapses (101.84 ± 16.70%, $p = 0.463$, $n = 6$), distal A/C-CA3 (102.07 ± 15.09%, $p = 0.753$, $n = 6$), and proximal A/C-CA3 (103.82 ± 6.18%, $n = 3$, $p = 0.593$) synapses. Representative traces for EPSPs and EPSCs at the three different synapses (Figure 1D1-1D3 and 1E1-1E3, respectively) demonstrate only PP-EPSPs were potentiated after the conditioning (red traces). These results indicate that the somatic repetitive firing induces potentiation of EPSPs at PP-CA3 synapses, but not at A/C-CA3 synapses.

2. Minimal stimulation at PP-CA3 synapses

Because the potentiation of PP-EPSPs by the conditioning was only observed from PP-CA3 synapses, I tested the possibility that the conditioning modulates LTP at PP-CA3 synapses. Minimal stimulation at PP-CA3 synapses was performed as described in Materials and Methods. Figure 2A

illustrates the averaged traces of EPSCs recorded in non-failure trials at different stimulation intensities. The averaged peak amplitude of EPSCs showed an abrupt increase at stimulus of 5.5 V (Figure 2B), and the amplitude of EPSCs were not significantly changed by a small (0.2 - 0.3 V) increase in the stimulus intensity. But stronger stimulation caused further increase in the amplitudes of EPSCs. Nevertheless, I found that individual amplitudes of EPSCs evoked every 10 s were not uniform between non-failure trials (Figure 2C), indicating the EPSCs are may not originate from a single synapse. The averaged peak amplitude of EPSCs evoked by minimal stimulation of PP was 9.58 ± 1.56 pA, and the failure rates were 52.75 ± 3.30%.

3. Relationship between LTP induction and stimulus intensity at PP-CA3 synapses

After establishment of minimal stimulation intensity of PP-CA3 synapses, I examined whether high frequency stimulation (HFS) of the PP at the minimal stimulation intensity induces LTP. HFS protocol consists of 10 bursts repeated at 0.1 Hz (Figure 3A1), with each bursts composed of 20 pulses at 100 Hz (Figure 3A2). Figure 3A1-3A2 depict the HFS protocol (black) and corresponding traces of voltage response (red). Before and after HFS of the PP, test pulses for monitoring EPSPs were delivered every 8 s. Amplitudes of EPSCs were assessed before HFS and 30 min after HFS at 0.1 Hz. At the end of each experiment, DCG-IV was applied to rule out the possibility of contamination by A/C inputs. When the PP was stimulated under the criteria

of minimal stimulation (thereafter termed weak HFS), E-S coupling did not occur during HFS (Figure 3A). In the time-dependent change of PP-EPSPs shows (Figure 3B), the weak HFS did not induce LTP of PP-EPSP (Figure 3B). Neither EPSC (3C1 and 3D1, 104.07 ± 10.92%, p = 0.889, n = 8) nor EPSP (3C2 and 3D2, 97.39 ± 9.20%, p = 0.889, n = 8) were altered by the weak HFS, indicating that LTP of PP-CA3 synapse is not induced by the weak HFS.

Next, I tested whether LTP can be induced by stronger stimulation which elicits EPSCs with the peak amplitude higher than 10 10.24 ± 1.64 pA (The Amplitude of baseline EPSC in stronger stimulation is 22.51 ± 4.46 pA, n = 5). To this end, I did the same experiments as in Figure 3 except that stronger stimulation intensity was adopted. During the strong HFS, E-S coupling was always observed (Figure 4A). Consistent with the Hebb's rule, LTP were observed after such strong HFS (Figure 4B). The overall HFS protocol and corresponding voltage traces were illustrated in Figure 4A1, and each burst protocol and elicited voltage traces were represented in Figure 4A2. Figure 4C1-4C2 shows averaged traces for PP-EPSC and PP-EPSP before and after strong HFS. The mean values for potentiation of EPSCs and EPSPs are summarized in Figure 4D1-4D2 (EPSC in 4D1, 379.86 ± 38.31%, p = 0.043, n = 5; EPSP in 4D, 312.55 ± 46.39%, p = 0.043, n = 5). Figure 4C1-4C2 shows averaged traces for PP-EPSC and PP-EPSP before and after strong HFS. The mean values for potentiation of EPSCs and EPSPs are summarized in Figure 4D1-4D2 (EPSC in 4D1, 379.86 ± 38.31%, p = 0.043, n = 5; EPSP

in 4D, 312.55 ± 46.39%, p = 0.043, n = 5).

4. The repetitive somatic firing lowers the threshold for LTP of PP-EPSCs

Above results show that the conditioning, which enhances the intrinsic excitability (Hyun et al, 2013), induces potentiation of EPSP only at PP-CA3 synapses. I tested whether the weak HFS of PP, which by itself does not induce LTP, can induce LTP of PP-EPSCs in CA3-PCs that are conditioned with repetitive somatic firing.

In the above experiments, EPSPs were monitored every 8 s, while EPSCs were evaluated at the start and the end of the EPSP monitoring. In Figure 1, I monitored EPSPs to investigate the effect of the conditioning on the synaptic responses at PP- and A/C-CA3 synapses. Because previous studies indicate that LTP is accompanied with an increase in the local excitability (Xu et al, 2005; Frick et al. 2004). I adopted EPSPs as an indicator for a change of synaptic property. However, given that EPSPs are influenced by voltage-gated ionic conductance (Urban et al, 1998; Hoffman et al. 1997; Magee, 1998; Kim et al, 2012). PP-EPSPs may undergo potentiation without a change of corresponding EPSCs. To rule out the influence of voltage-gated ionic conductance on the synaptic strength, I adopted EPSCs as indicators of synaptic currents and monitored continuously every 10 s in the experiment for Figure 5. However, because of the need for evaluation the conditioning effect, EPSPs were monitored intermittently. The baseline, EPSCs and EPSPs were

monitored for 120 sec and 80 sec, respectively. Stimulation intensities were adjusted such that the behaviour of EPSCs meets the criteria for minimal stimulation. After monitoring the baseline EPSCs, the CA3-PC was conditioned by somatic current injection under current clamp mode. Protocol and corresponding trace of conditioning were illustrated in the inset of Figure 5B. After the conditioning (blue arrowhead in Figure 5B), EPSCs were monitored for 6 minutes (Figure 5B). Figure 5D shows that PP-EPSCs were not altered by repetitive somatic firing, whereas EPSPs were potentiated. The weak HFS protocol was delivered to the PP pathway. The overall diagram of the HFS protocol (black) and corresponding voltage trace (red) are illustrated in Figure 5A1. Figure 5A2 depicts each burst protocol (black) and voltage trace as a response of protocol (red). As shown in Figure 3, the weak HFS was insufficient to induce LTP by itself. To prevent washout of intracellular milieu that is needed to induce LTP, the HFS protocol had to be delivered within 20 min after break-in (Malinow and Tsien, 1990). Distinct from un-conditioned CA3-PCs (Figure 3), E-S coupling was observed during the weak HFS of PP pathway in the conditioned CA3-PCs (Figure 5A). Moreover, the weak HFS readily induced LTP of PP-EPSCs in the same CA3-PCs (Figure 5B). This finding is in contrast to the lack of PP-EPSCs change by the weak HFS in un-conditioned PCs (Figure 3). This potentiation of EPSC was maintained at least 30 minutes. At 30 min after the HFS of PP pathway, PP-EPSPs were assessed. Figure 5D shows representative traces of EPSCs and EPSPs, and depicts the effects of conditioning (blue) and HFS protocol (red) in comparison with the

baseline traces (black). In figure 5E1-5E2, conditioning potentiated only EPSPs (157.26 ± 8.39%, p = 0.003, n = 9) with no change in the EPSCs (96.59 ± 4.82%, p = 0.739, n = 9). However, the weak HFS applied after the somatic conditioning potentiated both EPSPs (241.52 ± 19.94%, p = 0.003, n = 9) and EPSCs (229.90 ± 30.08%, p = 0.003, n = 9). Figure 5D summarizes mean values for the EPSCs and EPSPs amplitudes after conditioning and the subsequent weak HFS.

In Figure 6, the EPSC potentiation ratio, defined as ratio of the peak amplitude of EPSC at 30 min after HFS to the baseline EPSC, for individual cells were represented as a function of the baseline EPSC amplitude. For the PP-EPSCs evoked by semi-minimal stimulation protocol (black filled circle), the weak HFS did not induce LTP. In contrast, after the conditioning, the weak HFS was able to induce LTP (red filled circle). For the larger amplitude EPSCs evoked by stronger stimulus intensity (blue filled circle), the strong HFS induced LTP by itself.

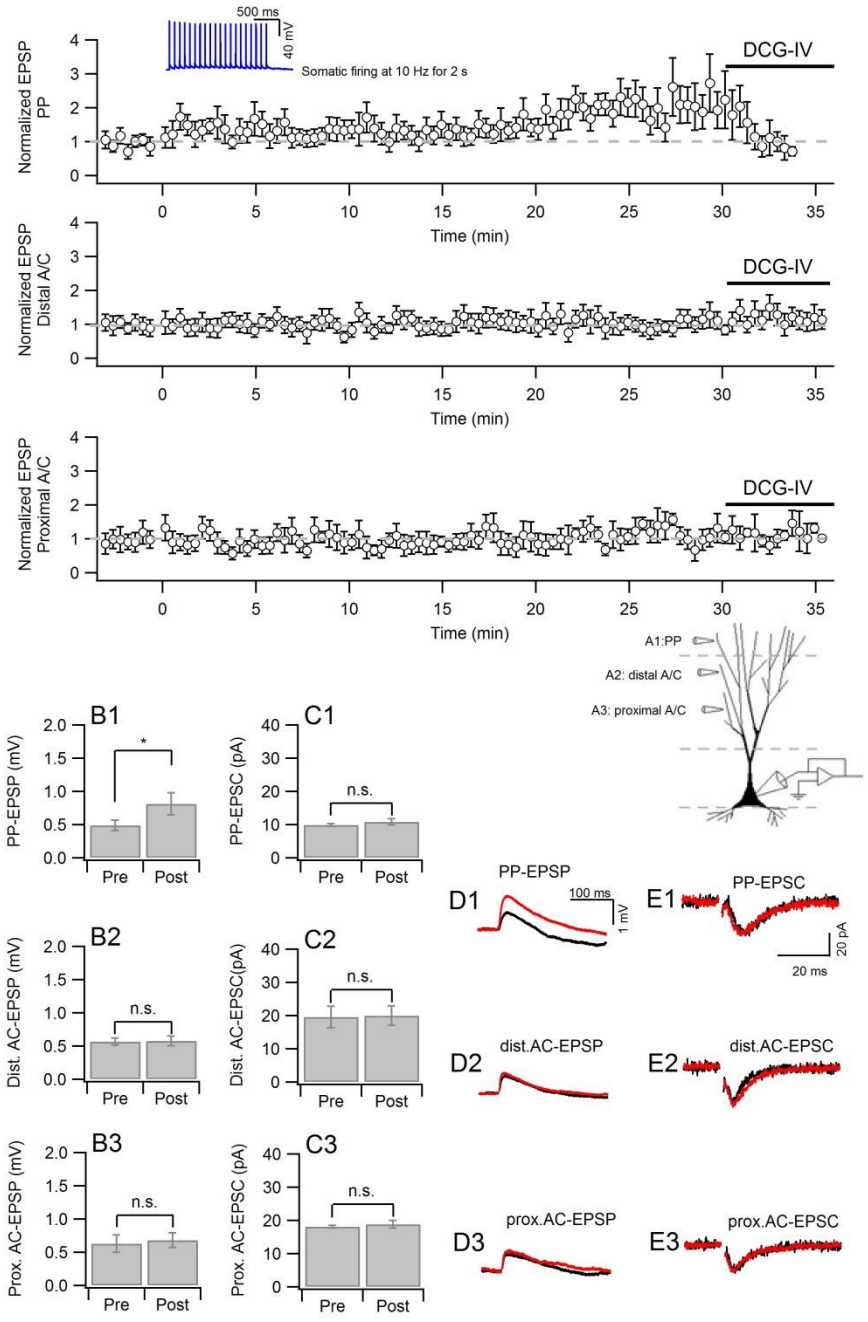

Figure 1 The effect of conditioning of the CA3-PCs with somatic repetitive firing on the EPSPs recorded at PP-CA3 synapses and A/C-CA3 synapses.

Figure 1 The effect of conditioning at PP-CA3 synapses and A/C-CA3 synapses. **A1**, Normalized EPSPs monitored at PP-CA3 synapses. After conditioning, potentiation of EPSPs occurred at PP-CA3 synapses. Blue arrowhead represents the time for conditioning. **A2-A3**, Normalized EPSPs monitored at distal (A2) and proximal (A3) A/C-CA3 synapses. Neither potentiation of EPSPs nor attenuation by DCG-IV was observed at A/C-CA3 synapses after conditioning. Figure inset of 1A represents corresponding voltage trace of conditioning protocol. Conditioning consists of repetitive somatic current injection at 10 Hz for 2 s. each current injection is amplitude of 1200 pA, duration of 2.2 ms. These are sufficient to evoke action potential. Figure inset below 1A3 is schematic diagram about position of electrodes for perforant path, distal A/C, proximal A/C. **B1-B3,** Amplitude of EPSPs before (Pre) and after 20 min (Post) were compared at PP-CA3 (B1), distal A/C-CA3 (B2), and proximal A/C-CA3 (B3). Only EPSPs of PP-CA3 was potentiated significantly (mean ± sem; Wilcoxon's signed rank-sum test, $p < 0.05$ denote as *, $p < 0.01$ denote as **, n.s. denotes not significant statistically). C1-C3, Amplitude of EPSCs before (Pre) and after 20 min (Post) were compared at PP-CA3 (C1), distal A/C-CA3 (C2), and proximal A/C-CA3 (C3). There is no significant change of EPSCs before and after priming (mean ± sem; Wilcoxon's signed rank-sum test, $p < 0.05$ denote as *, $p < 0.01$ denote as **, n.s. denotes not significant statistically). **D1**-**D3**, Represent traces for comparison of EPSPs before (black) and after 20 min (red) at PP-CA3 (E1), distal A/C-CA3 (E2), and proximal A/C-CA3 (E3). Potentiation of EPSPs was

observed only PP-CA3 synapses after priming**. E1-E3**, Represent traces for comparison of EPSCs before (black) and after 20 min (red) at PP-CA3 (E1), distal A/C-CA3 (E2), and proximal A/C-CA3 (E3).

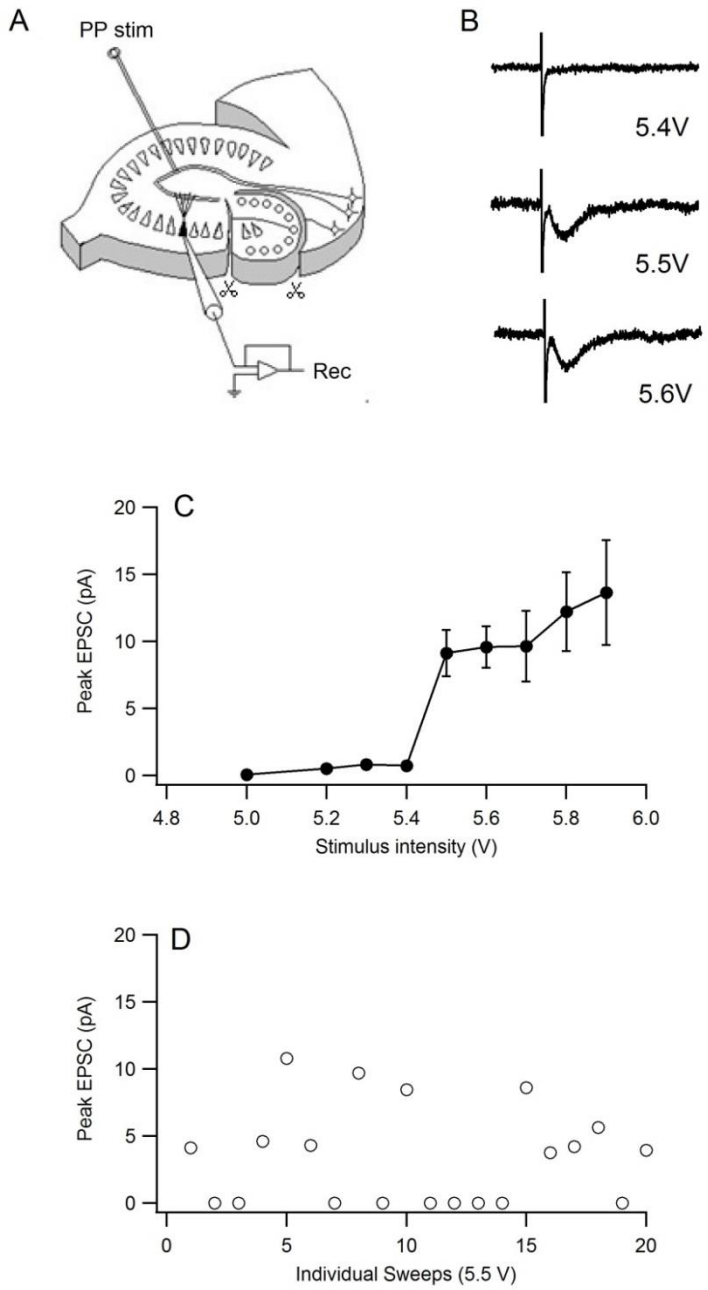

Figure 2 Minimal stimulation for PP-CA3 synapses and unitary EPSCs in CA3 pyramidal neurons.

Figure 2 Minimal stimulation for PP-CA3 synapses and unitary EPSCs in CA3 pyramidal neurons. **A**, Concentric bipolar electrode was placed in CA3 stratum lacunosum-moleculare of a slice incised along the sulcus hippocampi and across the edge of the dentate molecular layer, and across the hilum of hippocampus (represented as scissors). **B,** EPSCs elicited by extracellular stimulation of perforant pathway through concentric bipolar electrode. Each trace represents the average of 20 responses in corresponding stimulation intensity. **C,** Peak amplitude of stimulus-evoked EPSCs as a function of stimulation intensity. There is abrupt appearance of EPSCs with stimulus between 5.4 and 5.6 V, indicating stimulation of one or a few axon. **D**, Peak amplitude of evoked EPSCs at stimulus of 5.5 V as a function of time from one CA3-PC. Stimuli to evoke EPSCs were delivered every 10 s, and EPSCs were elicited with failure rates of 45%.

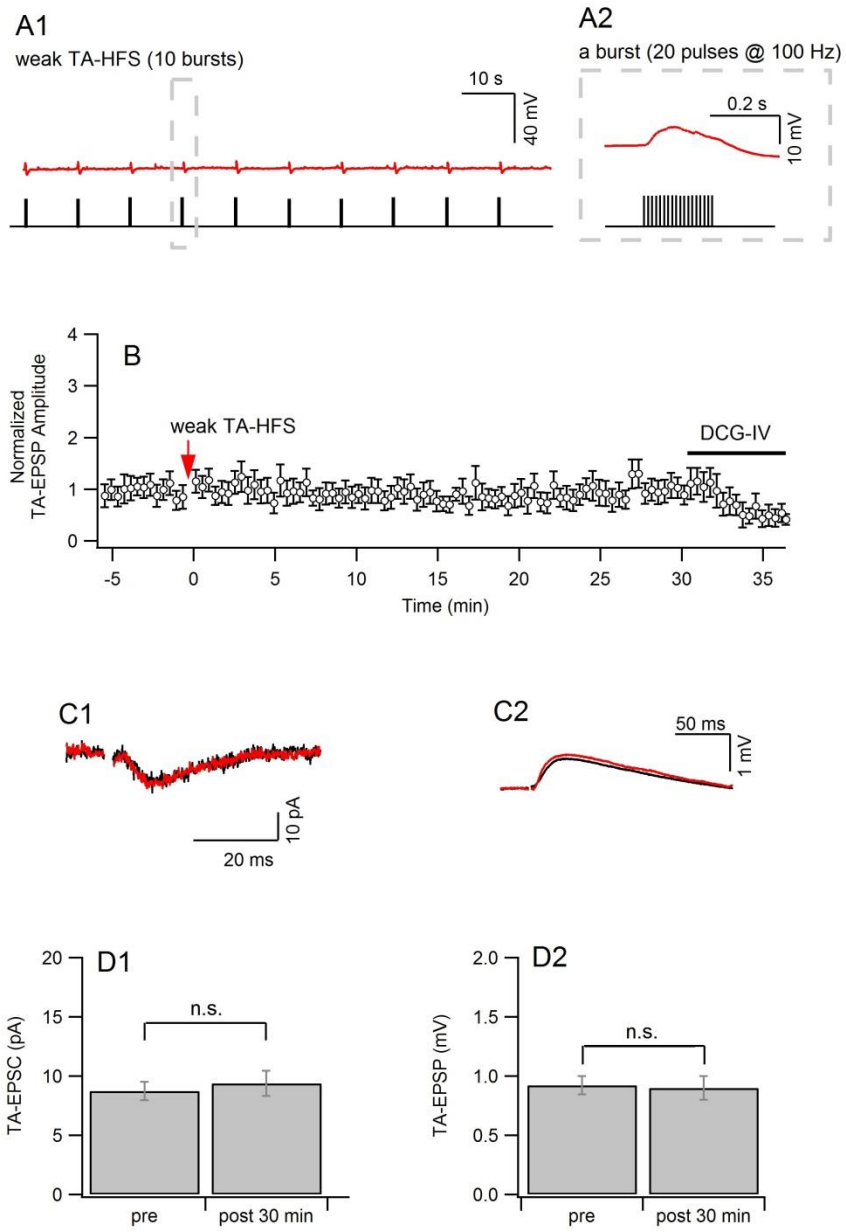

Figure 3 weak HFS at PP-CA3 synapses is insufficient to induce LTP. **A1-A2**, Diagram (black) and response (red) of weak HFS.

Figure 3 weak HFS at PP-CA3 synapses is insufficient to induce LTP. **A1-A2**, Diagram (black) and response (red) of weak HFS. HFS consisted of 10 bursts delivered per 10 s (A1), and each bursts consisted of 20 stimuli at 100 Hz (A2, corresponded to gray-dashed line box of A1). This HFS protocol was applied at -60 mV, adjusted in current-clamp mode. **B**, Normalized EPSPs monitored at PP-CA3 synapses. After HFS, no potentiation of EPSPs occurred at PP-CA3 synapses, and EPSPs attenuated by application of DCG-IV by 75%. **C1-C2**, Represent traces for comparison of EPSCs (C1) and EPSPs (C2) before (black) and after 30 min (red) at PP-CA3 synapses. Neither EPSCs nor EPSPs changed after HFS compared to before HFS. **D1-D2**, Amplitude of EPSCs (D1) and EPSPs (D2) before (Pre) and after 30 min (Post) were compared at PP-CA3. There is no significant change of EPSCs and EPSPs before and after HFS (mean ± sem; Wilcoxon's signed rank-sum test, $p < 0.05$ denote as *, $p < 0.01$ denote as **, n.s. denotes not significant statistically).

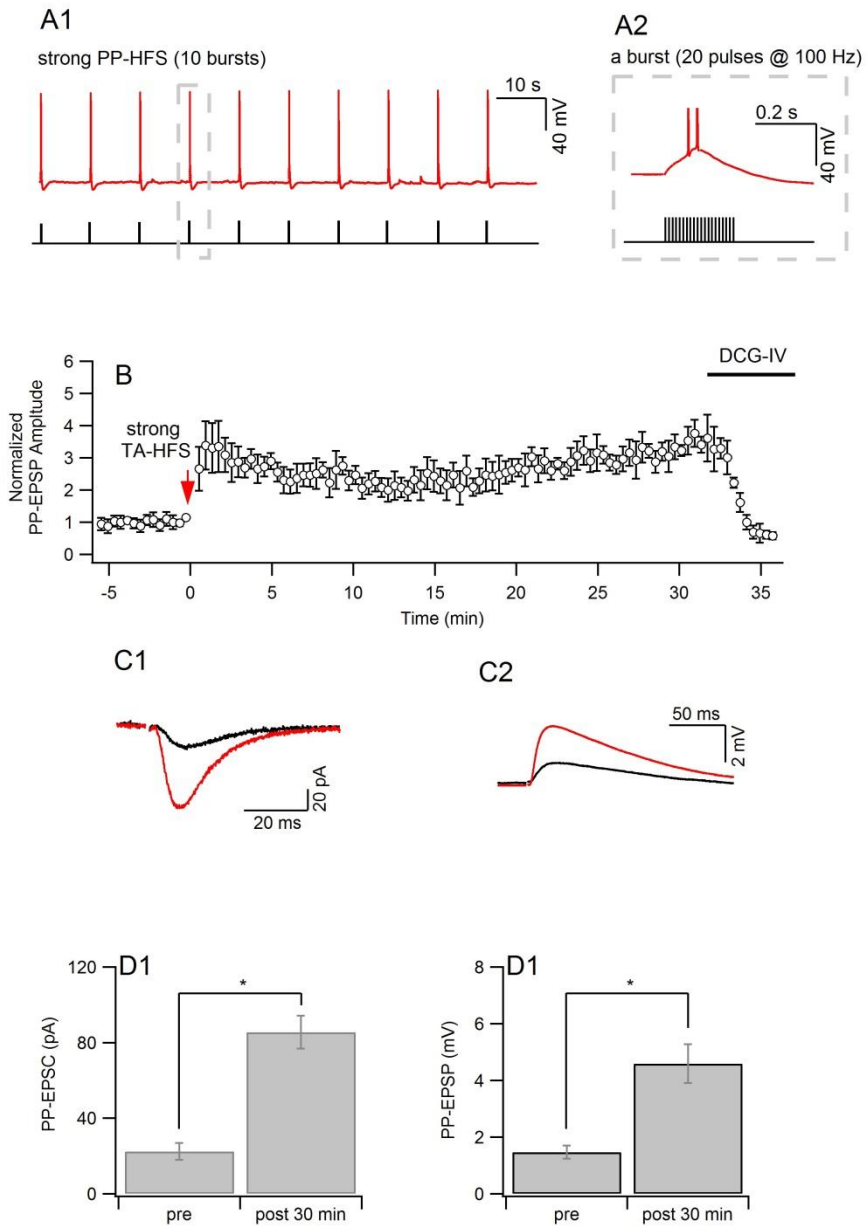

Figure 4 strong HFS at PP-CA3 synapses is sufficient to induce LTP itself.

Figure 4 strong HFS at PP-CA3 synapses is sufficient to induce LTP itself. **A1-A2**, Diagram (black) and response (red) of weak HFS. HFS consisted of 10 bursts delivered per 10 s (A1), and each bursts consisted of 20 stimuli at 100 Hz (A2, corresponded to gray-dashed line box of A1). This HFS protocol was applied at -60 mV, adjusted in current-clamp mode. Note action potentials (APs) occurred by HFS, compare Figure 3A which APs not occurred. **B**, Normalized EPSPs monitored at PP-CA3 synapses. Red arrow indicates the time of delivering HFS. After HFS, robust potentiation of EPSPs occurred at PP-CA3 synapses, and EPSPs attenuated by application of DCG-IV by 75%. **C1-C2**, Represent traces for comparison of EPSCs (C1) and EPSPs (C2) before (black) and after 30 min (red) at PP-CA3 synapses. Both EPSCs and EPSPs changed after HFS compared to before HFS, in strong HFS. **D1-D2**, Amplitude of EPSCs (D1) and EPSPs (D2) before (Pre) and after 30 min (Post) were compared at PP-CA3. There is significant potentiation of EPSCs and EPSPs before and after priming (mean ± sem; Wilcoxon's signed rank-sum test, $p < 0.05$ denote as *, $p < 0.01$ denote as **, n.s. denotes not significant statistically).

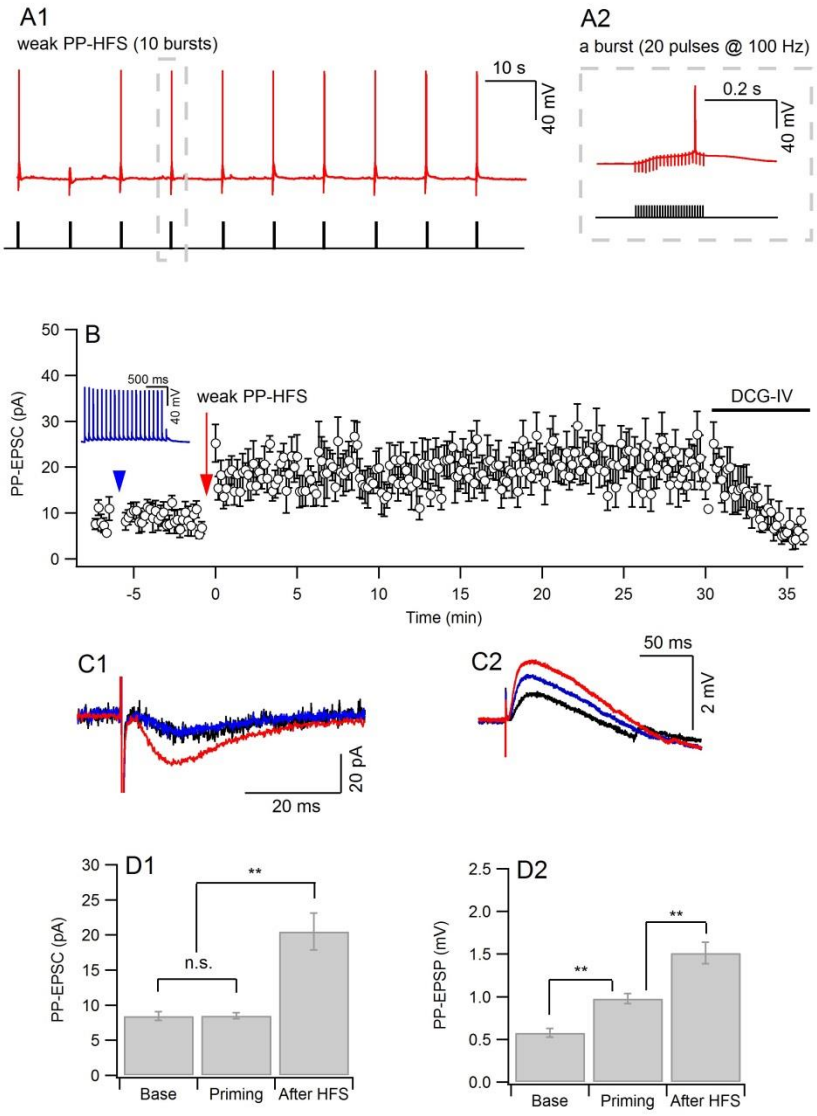

Figure 5 LTP can be induced by weak HFS after conditioning.

Figure 5 LTP can be induced by weak HFS after conditioning. Diagram of conditioning is illustrated in gray-dashed box. Priming consists of repetitive somatic current injection at 10 Hz for 2 s. each current injection is amplitude of 1200 pA, duration of 2.2 ms. The time of conditioning was indicated with blue arrowhead. **A1-A2**, Diagram (black) and response (red) of weak HFS. HFS consisted of 10 bursts delivered per 10 s (A1), and each bursts consisted of 20 stimuli at 100 Hz (A2, corresponded to gray-dashed line box of A1). This HFS protocol was applied at -60 mV, adjusted in current-clamp mode. The time of HFS protocol applied was depicted with red arrow. The stimulation intensity of this HFS is sub-threshold, which is insufficient to induce LTP without conditioning (Refer Figure 3). **B,** EPSCs were monitored at PP-CA3 synapses. Potentiation of EPSPs occurred after conditioning (refer Figure 5C), but not EPSCs. After conditioning, LTP was induced by weak HFS, represented in Figure 5B. EPSCs were attenuated by application of DCG-IV. **C1-C2.** Represent traces for comparison of EPSCs (C1) and EPSPs (C2) baseline (black), after priming (blue), and after HFS (red). Note EPSPs were potentiated by priming, but EPSCs were not. After LTP by HFS, both EPSCs and EPSPs were potentiated. **D1-D2**, Amplitude of EPSCs (E1) and EPSPs (E2) baseline (black), after priming (blue), and after HFS (red) were compared at PP-CA3. (mean ± sem; Friedman's test, $p < 0.05$ denote as *, $p < 0.01$ denote as **, n.s. denotes not significant statistically).

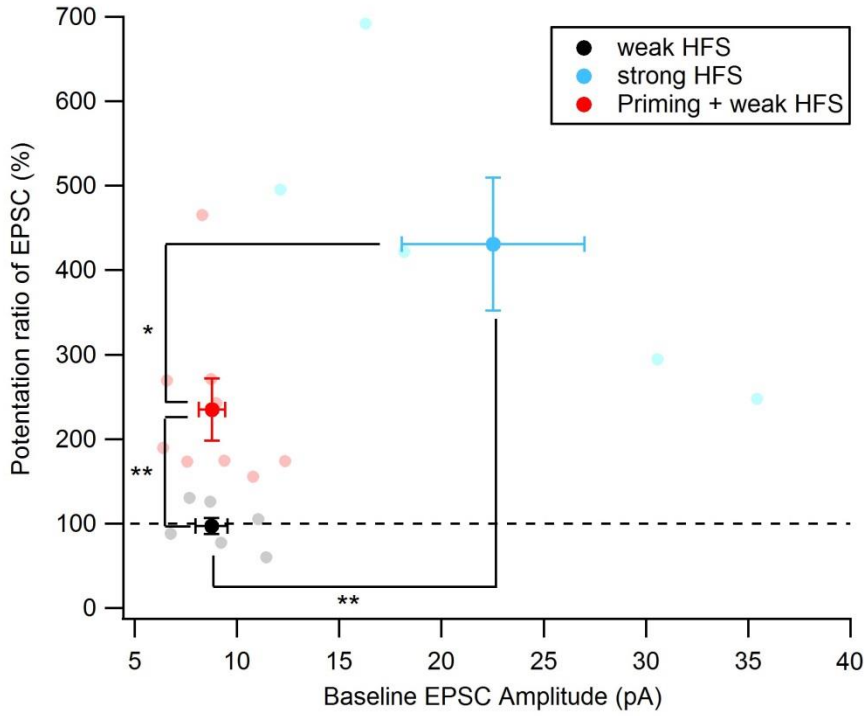

Figure 6 Metaplasticity of PP-CA3 synapses by conditioning composed of repetitive somatic current injection.

Figure 6 Metaplasticity of PP-CA3 synapses by conditioning composed of repetitive somatic current injection. After conditioning described above, properties of PP-CA3 synapses were changed to induce LTP easily. Each individual data for one category (weak HFS, strong HFS, and conditioning + weak HFS) was represented by pale-colored circle. (mean ± sem; Mann-Whitney's *U* test, $p < 0.05$ denote as *, $p < 0.01$ denote as **, n.s. denotes not significant statistically).

DISCUSSION

1. EPSPs of CA3-PC dendrites and the influence of somatic firing at 10 Hz

The present study shows the potentiation of EPSPs after the conditioning is specific for the PP-CA3 synapses. Moreover, EPSCs were potentiated neither at PP-CA3 nor at A/C-CA3 synapses. These results suggest that the potentiation of PP-EPSPs may not result from an increase in synaptic current but from dendritic excitability changes.

The amplitudes of PP-EPSPs and A/C-EPSPs are influenced by the activation of voltage-gated conductance. Urban et al. (1998) reported that PP-EPSPs were amplified by tetrodoxin-sensitive sodium currents and low-voltage activated calcium channels. In neocortical pyramidal neurons, the Na^+-mediated boosting during repetitive firing compensates electrotonic attenuation (Oviedo and Reyes, 2002). Recently, Kim et al. (2012) discovered that dendritic Na^+ spikes are effectively initiated at distal dendrites of CA3-PC by waveforms mimicking synaptic events, and distal dendrites of CA3-PC is ideal for backpropagation of action potentials and dendritic spike initiation because of high Na^+-to-K^+ conductance density ratio.

Dendritc A-type K^+ current attenuates the amplitude of EPSP and prevents initiation of action potentials in the dendrites (Hoffman et al. 1997). Hyperpolarization-activated current (I_h) dampens dendritic excitability in the subthreshold range of membrane potential in CA1 pyramidal cells (Magee, 1998). The D-type K^+ current is fast-activating, slow-inactivating, and

dendrotoxin-sensitive outward currents. It was characterized in hippocampal CA3 pyramidal cells (Lüthi et al. 1996) and CA1 pyramidal cells (Storm, 1988). The kinetic properties of D-type K^+ current contribute to a delay and variability in the first onset of action potential induced by current injection (Cudmore et al, 2010). Downregulation of D-type K^+ current by low concentration of 4-aminopyridine (4-AP) enhances membrane excitability in layer 5 pyramidal cells in rat neocortex (Bekker and Delaney, 2001). For pavalbumin-positive basket cells in hippocampal CA1 region, synaptic activation via activation of metabotropic glutamate receptor subtype 5 (mGluR5) induces downregulation of Kv1 channel activity and enhancement of LTP-IE (Campanac et al, 2013). And repetitive somatic current injection (suprathreshold current injection 10Hz, for 2s, same as conditioning protocol of author's study) downregulates D-type K^+ current subtype Kv1.2 and enhances membrane excitability (Hyun et al. 2013). In computer simulation model, role of D-type K^+-current for synaptic integration in model dendrites was predicted. For EPSP slopes monitored at 600 μm away from input site, presence of D-type K^+ current reduces amplitude of EPSP by 11% in comparison with passive model (Takagi et al, 1998). Considering the downregulation of D-type K current after repetitive somatic current injection and simulation model that predicts the role of D-type K^+ current for EPSP slopes in previous studies, potentiation of PP-EPSPs after conditioning in author's study may be explained by downregulation of D-type K^+ currents after conditioning. In this study, only PP-EPSPs potentiated after conditioning.

Previous report exhibits that surface expression of D-type K^+ current subunit Kv1.2 might be higher in the distal dendrites of CA3-PCs than the proximal dendrites of these (Hyun et al, 2013). The potentiation of EPSPs that only occurred in PP-CA3 synapses after conditioning (Fig. 1) can be explained by the heterogeneity of surface expression of D-type K^+-current, as previously reported.

2. Role of conditioning in the metaplasticity

After the conditioning, the increase in the amplitude of EPSP persisted at least 30 min. It has been reported that synaptic plasticity is modulated after conditioning using synaptic or non-synaptic electrical stimulation and pharmacological activation. Huang et al (1992) reported that after repetitive weak tetanus (0.15s / 30 Hz) suppresses strong tetanus (0.5s / 100 Hz)-induced LTP in an NMDA receptor-dependent manner. NMDA receptor-dependent conditioning also mediates facilitation of LTD. Holland and Wagner (1998) reported that low frequency stimulation (1 Hz / 10 min) induces higher magnitude of LTD after pre-conditioning HFS (two times of three bursts of 100 Hz / 1 s every 20 s), which does not induce any long-term synaptic change by itself.

Since both LTP and LTD were depolarization-dependent events, activity-dependent alternations of the properties of voltage-gated ionic conductance might regulate the induction of LTP and LTD (Zhang and Linden, 2003; Magee and Johnston, 2005; Sah and Bekkers, 1996). Such alternations of

voltage-gated ionic conductance were termed ‘intrinsic plasticity’. Intrinsic plasticity not only contributes to memory formation but also is a mechanism underlying induction of metaplasticity. Phamacological activation of group I metabotropic glutamate receptors (mGluR1) in neocortical neuron (Sourdet et al, 2003) and hippocampal neuron (Ireland and Abraham, 2002) elicits long-lasting reductions of AHP by the downregulation of Ca^{2+}-dependent K^+-channels. The degree of LTP was increased after the activation of mGluR5 in hippocampal pyramidal neuron (Cohen et al. 1999). Inhibition of A-type K^+-current by arachidonic acid enhances EPSPs and reduces the threshold of LTP in hippocampal CA1 pyramidal neuron (Ramakers and Storm, 2002).

Glutamate receptor stimulation by application of AMPA induces clathrin-mediated internalization of Kv4.2, and LTP induction by brief glycine application causes not only synaptic insertion of GluR1 subunit, but internalization of Kv4.2 (Kim et al, 2007). And in rat hippocampal slices, LTP induction was accompanied by local increase of dendritic excitability, which is mediated by hyperpolarized shift in inactivation curve of A-type K^+-currents (Frick et al, 2005). Hippocampal CA1 pyramidal neuron in organotypic hippocampal slices that are over-expressing of A-type K^+ channels and in acute hippocampal slices obtained from $Kv4.2^{-/-}$ mice exhibited a change of synaptic NMDA receptors subunit composition (NR2B/NR2A), which resulted in the inhibition or enhancement of LTP (Jung et al. 2008).

Aforementioned studies discuss homosynaptic metaplasticity; that is, the

synapses that are previously activated by priming action also exhibit altered synaptic plasticity. However, alteration of synaptic plasticity can be induced by activation of neighbouring synapses by priming action. Such phenomenon termed ‘heterosynaptic metaplasticity’. In dentate gyrus, when LTP is induced at medial perforant path afferents, the induction of LTP of lateral perforant path was inhibited in *vivo* (Abraham et al. 2001). Hunt et al. (2013) reported that heterosynaptic metaplasticity between A/C synapses and mossy fiber synapses is mediated by NMDA receptors of mossy fibers. However, the metaplasticity of PP-CA3 synapses has not been investigated. The present study is the first report that the metaplasticity of PP-CA3 synapse can be induced by the somatic conditioning to the best author’s knowledge. However, this study has limitations in that the property of LTP is not characterized in terms of dependency of NMDA receptors and the property of change of ionic conductance that subserves the amplification of PP-EPSPs.

The postsynaptic AP firing during the HFS of PP is the common feature for both in the LTP induction by the strong HFS of PP in naïve CA3-PCs (Figure 4A) and that by the weak HFS applied subsequent to the conditioning (Figure 5A). The weak HFS of PP induced no postsynaptic APs in naïve CA3-PCs (Figure 3). However, in the CA3-PCs that were conditioned with repetitive somatic current injection, the amplitudes of PP-EPSPs were increased and postsynaptic APs occurred on the top of the temporal summation of PP-EPSPs. The previous study indicates that LTP of PP-CA3 synapses are NMDA receptor-dependent (McMahon and Barrionuevo, 2002). Once PP-EPSPs is

augmented by the conditioning, weak HFS will be sufficient to induce AP firing in the post-synaptic CA3-PC, and induce LTP by providing the sufficient post-synaptic depolarization for activating NMDA receptors. Considering previous studies about D-type K^+ currents in intrinsic excitability (Hyun et al, 2013) of CA3-PC and A-type K^+ currents in metaplasticity of LTP in CA1 pyramidal neuron (Jung et al, 2008), dendritic K^+ currents in the pyramidal cells might be an important regulator determining the threshold of LTP induction.

3. Functional implications of somatic firing-induced metaplasticity

Environmental stimuli and learning can cause a change of intrinsic excitability in cortical neurons, which is associated with metaplasticity of synaptic inputs to the neuron. Intensively stressful environment, such as restraint and tail shock, inhibits the hippocampal LTP induction and facilitates the LTD induction. These modulations of synaptic plasticity lasted up to 24 hours after stress, and blocked by systemic NMDA-R antagonists at time of the stress (Kim et al, 1996). In vertebrates, reflex conditioning is able to cause the plasticity of cellular excitability. After the eye-blink conditioning in the rabbit, the decrease of slow AHP and the increase of cell firing in hippocampal CA1 pyramidal cells lasted up to 5 days after conditioning (Moyer et al, 1996). Similar effects were observed in the rat CA1 pyramidal cells after Morris water maze training (Oh et al, 1996). After olfactory-discrimination training in mice, AHP of hippocampal pyramidal neuron was decreased, indicative of

mGluR-mediated metaplastic facilitation of LTP (Saar et al, 1998).

The role of MF-CA3 synapse was predicted as detonator synapse, in that it always produces intensive depolarization and firing of CA3-PCs. (McNaughton and Morris, 1987; Henze, 2000). And Henze et al. (2002) represented the evidence about monoquntal property of giant miniature EPSCs (mEPSCs) of MF synapse, and the firing ability of giant mEPSCs of MF synapses to CA3-PCs. Dentate gyrus (DG) has been believed as a possible source of neuronal pattern separation, and Leutgeb et al. (2007) showed that minimal changes in the shape of the surrounding environment can induce alteration of activity-patterns among place-modulated granule cells in the DG. Taken together, the activity-dependent metaplasticity of direct cortical inputs at PP-CA3 synapses by repetitive somatic firing in this study may enhance the pattern separation ability in minimal changes of surround environment, without interference of pattern completion.

REFERENCES

Abraham WC. (2008). "Metaplasticity: tuning synapses and networks for plasticity." Nat Rev Neurosci **9**(5):387-399.

Abrahan WC, Bear, MF. (1996). "Metaplasticity: the plasticity of synaptic plasticity." Trends Neurosci **19**:126-130.

Abraham WC, Mason-Parker SE, et al. (2001). "Heterosynaptic metaplasticity in the hippocampus in vivo: a BCM-like modifiable threshold for LTP." Proc Natl Acad Sci USA.**98**(19):10924-9.

Andersen P, Sundberg SH, et al (1980). "Possible mechanisms for long-lasting potentiation of synaptic transmission in hippocampal slices from guinea-pigs." J Physiol. **302**:463-82.

Baker JL, Perez-Rosello T, et al. (2010). "A computer model of unitary responses from associational/commissural and perforant path synapses in hippocampal CA3 pyramidal cells." J Comput Neurosci. **31**(1):137-58.

Brager DH, Johnston D. (2007). "Plasticity of intrinsic excitability during long-term depression is mediated through mGluR-dependent changes in I(h) in hippocampal CA1 pyramidal neurons." J Neurosci. **27**(51):13926-37.

Campanac E, Debanne D. (2007). "Plasticity of neuronal excitability: Hebbian rules beyond the synapse." Arch Ital Biol. **145**(3-4):277-87.

Campanac E, Gasselin C, et al. (2013). "Enhanced intrinsic excitability in basket cells maintains excitatory-inhibitory balance in hippocampal

circuits." Neuron. **77**(4):712-22.

Chavez-Noriega LE, Bliss TV, et al. (1989). "The EPSP-spike (E-S) component of long-term potentiation in the rat hippocampal slice is modulated by GABAergic but not cholinergic mechanisms." Neurosci Lett. **104**(1-2):58-64.4

Claiborne, BJ, Amaral DG, et al. (1986). "A light and electron microscopic analysis of the mossy fibers of the rat dentate gyrus." J Comp Neurol. 246:435–458.

Cohen AS, Coussens CM, et al. (1999). "Long-lasting increase in cellular excitability associated with the priming of LTP induction in rat hippocampus." J Neurophysiol. **82**(6):3139-48.

Cudmore RH, Fronzaroli-Molinieres L, et al. (2010). "Spike-time precision and network synchrony are controlled by the homeostatic regulation of the D-type potassium current." J Neurosci. **30**(38):12885-95.

Daoudal G, Debanne D. (2003). "Long-term plasticity of intrinsic excitability: learning rules and mechanisms." Learn Mem. **10**(6):456-6.

Dobrunz LE, Huang EP, et al. (1997). "Very short-term plasticity in hippocampal synapses." Proc Natl Acad Sci U S A. **94**:14843-14847.

Ferbinteanu J, Holsinger RM, et al. (1999). "Lesions of the medial or lateral perforant path have different effects on hippocampal contributions to place learning and on fear conditioning to context." Behav Brain Res. **101**(1):65-84.

Frick A, Magee J, et al. (2004). "LTP is accompanied by an enhanced local

excitability of pyramidal neuron dendrites." Nat Neurosci. **7**(2):126-35.

Hasselmo ME, Schnell E, et al. (1995). "Dynamics of learning and recall at excitatory recurrent synapses and cholinergic modulation in rat hippocampal region CA3." J Neurosci. **15**(7):5249-62.

Henze DA, Urban NN, et al. (2000), "The multifarious hippocampal mossy fiber pathway: a review." Neuroscience. **98**(3):407-27.

Henze DA, McMahon DB et al. (2002), "Giant miniature EPSCs at the hippocampal mossy fiber to CA3 pyramidal cell synapse are monoquantal." J Neurophysiol. **87**(1):15-29.

Hoffman DA, Magee JC, et al. (1997) "K^+ channel regulation of signal propagation in dendrites of hippocampal pyramidal neurons." Nature. **387**(6636):869-75.

Holland LL, Wagner JJ. (1998). "Primed facilitation of homosynaptic long-term depression and depotentiation in rat hippocampus." J Neurosci. **18**(3):887-94.

Huang YY, Colino A, et al. (1992). "The influence of prior synaptic activity on the induction of long-term potentiation." Science. **255**(5045):730-3.

Hunsaker MR, Mooy GG, et al. (2007). "Dissociations of the medial and lateral perforant path projections into dorsal DG, CA3, and CA1 for spatial and nonspatial (visual object) information processing."

Behav Neurosci. **121**(4):742-50.

Hunt DL, Puente N, et al. (2013). "Bidirectional NMDA receptor plasticity controls CA3 output and heterosynaptic metaplasticity." Nat Neurosci. **16**(8):1049-59.

Hyun JH, Eom K, et al. (2013). "Activity-dependent downregulation of D-type K^+ channel subunit Kv1.2 in rat hippocampal CA3 pyramidal neurons." J Physio. PMID: 23981714.

Ireland DR, Abraham WC. (2002). "Group I mGluRs increase excitability of hippocampal CA1 pyramidal neurons by a PLC-independent mechanism." J Neurophysiol. 88(1):107-16.

Ishizuka N, Weber J, et al. (1990). "Organization of intrahippocampal projections originating from CA3 pyramidal cells in the rat." J Comp Neurol. **295**(4):580-623.

Kesner RP. (2007). "Behavioral functions of the CA3 subregion of the hippocampus." Learn Mem. 14(11):771-81.

Kazu Nakazawa, Nichel C. Quirk, et al. (2002) "Requirement for hippocampal CA3 NMDA receptors in associational memory recall." Science. **297**(5579):211-8.

Kim J, Jung SC, et al. (2007). "Regulation of dendritic excitability by activity-dependent trafficking of the A-type K^+ channel subunit Kv4.2 in hippocampal neurons." Neuron. **54**(6):933-47.

Kim JJ, Foy MR, et al. (1996). "Behavioral stress modifies hippocampal plasticity through N-methyl-D-aspartate receptor activation." Proc

Natl Acad Sci U S A. **93**(10):4750-3.

Kim S, Guzman SJ, et al. (2012). "Active dendrites support efficient initiation of dendritic spikes in hippocampal CA3 pyramidal neurons." Nat Neurosci. **15**(4):600-6.

Lee D, Lee KH, et al. (2007). "Target cell-specific involvement of presynaptic mitochondria in post-tetanic potentiation at hippocampal mossy fiber synapses." J Neurosci. **27**(50):13603-13.

Leutgeb J, Leutgeb S, et al. (2007). "Pattern separation in the Dentate Gyrus and CA3 of the Hippocampus." Science. **315**(5814):961-6.

Lynch MA, Clements MP, et al. (1988). "Increased hydrolysis of phosphatidylinositol-4,5-bisphosphate in long-term potentiation." Neurosci Lett. **84**(3):291-6.

Lüthi A, Gähwiler BH, et al. (1996). "A slowly inactivating potassium current in CA3 pyramidal cells of rat hippocampus in vitro." J Neurosci. **16**(2):586-94.

Jung SC, Kim J, et al. (2008). "Rapid, bidirectional remodeling of synaptic NMDA receptor subunit composition by A-type K^+ channel activity in hippocampal CA1 pyramidal neurons." Neuron. **60**(4):657-71.

Magee JC. (1998). "Dendritic hyperpolarization-activated currents modify the integrative properties of hippocampal CA1 pyramidal neurons." J Neurosci. **18**(19):7613-24.

Magee JC, Johnston D. (2005). "Plasticity of dendritic function." Curr Opin Neurobiol. **15**(3):334-42.

Malinow R, Tsien RW. (1990) “Presynaptic enhancement shown by whole-cell recordings of long-term potentiation in hippocampal slices.” Nature. **346**(6280):177-80.

Martin SJ, Grimwood PD, et al. (2000). “Synaptic plasticity and memory: an evaluation of the hypothesis.” Annu. Rev. Neurosci. **23**:649-711.

Martinez CO, Do VH, et al. (2002). “Associative long-term potentiation (LTP) among extrinsic afferents of the hippocampal CA3 region in vivo.” Brain Res. **940**(1-2):86-94.

McMahon DB, Barrionuevo G. (2002). “Short- and long-term plasticity of the perforant path synapse in hippocampal area CA3.” J Neurophysiol. **88**(1):528-33.

McNaughton BL, Morris RG. (1987). “Hippocampal synaptic enhancement and information storage within a distributed memory system.” Trends Neurosci. 10:408-415.

Mockett B, Coussens C, et al. (2002). “NMDA receptor-mediated metaplasticity during the induction of long-term depression by low-frequency stimulation.” Eur J Neurosci. **15**(11):1819-26.

Moyer JR Jr, Thompson LT, et al. (1996). “Trace eyeblink conditioning increases CA1 excitability in a transient and learning-specific manner.” J Neurosci. **16**(17):5536-46.

Oh MM, Kuo AG, et al. (2003). “Watermaze learning enhances excitability of CA1 pyramidal neurons.” J Neurophysiol. **90**(4):2171-9.

Oviedo H, Reyes AD. (2002). “Boosting of neuronal firing evoked with

asynchronous and synchronous inputs to the dendrite." Nat Neurosci. **5**(3):261-6.

Ramakers GM, Storm JF. (2002). "A postsynaptic transient K(+) current modulated by arachidonic acid regulates synaptic integration and threshold for LTP induction in hippocampal pyramidal cells." Proc Natl Acad Sci U S A. **99**(15):10144-9.

Raastad M. (1995). "Extracellular activation of unitary excitatory synapses between hippocampal CA3 and CA1 pyramidal cells." Eur J Neurosci. **7**:1882-1888.

Saar D, Grossman Y, et al. (1998). "Reduced after-hyperpolarization in rat piriform cortex pyramidal neurons is associated with increased learning capability during operant conditioning." Eur J Neurosci. **10**(4):1518-23.

Sah P, Bekkers JM. (1996). "Apical dendritic location of slow afterhyperpolarization current in hippocampal pyramidal neurons: implications for the integration of long-term potentiation." J Neurosci. **16**(15):4537-42.

Sehgal M, Song C, et al. (2013). "Learning to learn - Intrinsic plasticity as a metaplasticity mechanism for memory formation." Neurobiol Learn Mem. **105**:186-99.

Sourdet V, Russier M, et al. (2003). "Long-term enhancement of neuronal excitability and temporal fidelity mediated by metabotropic glutamate receptor subtype 5." J Neurosci. **23**(32):10238-48.

Stafekhina VS, Vinogradova OS. (1978). “Characteristics of the hippocampal cortical input. Functional differences between lateral and medial entorhinal areas.” Neurosci Behav Physiol. **9**:8-14

Steward O. Topographic organization of the projections from the entorhinal area to the hippocampal formation of the rat. J Comp Neurol. 1976 Jun 1;167(3):285-314..

Stoop R, Conquet F, et al. (2003). “Activation of metabotropic glutamate 5 and NMDA receptors underlies the induction of persistent bursting and associated long-lasting changes in CA3 recurrent connections.” J Neurosci. 23(13):5634-44.

Storm JF. (1988). “Temporal integration by a slowly inactivating K^+ current in hippocampal neurons.” Nature. **336**(6197):379-81.

Takagi H et al. (1998). “Roles of A- and D-type K channels in EPSP integration at a model dendrite.” Neurosci Lett.**254**:165-8.

Thiels E, Barrionuevo G, Berger TW. (1994). “Excitatory stimulation during postsynaptic inhibition induces long-term depression in hippocampus in vivo.” J Neurophysiol. **72**(6):3009-16.

Treves A, Rolls ET. (1994). “Computational analysis of the role of the hippocampus in memory.” Hippocampus. **4**(3):374-391.

Tsukamoto M, Takuya Y (2003). “Mossy fibre synaptic NMDA receptors trigger non-Hebbian long-term potentiation at entorhino-CA3 synapses in the rat.” J Physio. **546**(3):665-675.

Urban NN, Henze DA, et al. (1998). “Amplification of perforant-path EPSPs

in CA3 pyramidal cells by LVA calcium and sodium channels." J Neurophysiol. **80**(3):1558-61.

Vazdarjanova A, Guzowski JF. (2004). "Differences in Hippocampal Neuronal Population Responses to Modifications of an Environmental Context: Evidence for Distinct, Yet Complementary, Functions of CA3 and CA1 Ensembles." J Neurosci. **24**(29):6489-96.

Witter MP, Amaral DG. (1991). "Entorhinal cortex of the monkey: V. Projections to the dentate gyrus, hippocampus, and subicular complex." J Comp Neurol. **307**(3):437-59.

Xu J, Kang N, et al. (2005). "Activity-Dependent Long-Term Potentiation of Intrinsic Excitability in Hippocampal CA1 Pyramidal Neurons." J Neurosci. **25**(7):1750-1760.

Zhang W, Linden DJ. (2003). "The other side of the engram: experience-driven changes in neuronal intrinsic excitability." Nat Rev Neurosci. **4**(11):885-900.

국문 초록

신경세포의 내재적 흥분성은 기억의 부호화 및 시냅스를 통한 입력과 활동전압 형성의 연결에 있어 중요한 역할을 수행한다. 생리학적으로 적절한 빈도수의 반복적인 신경세포체에서의 활동전압 발생은 고유해마의 CA3 영역의 추체세포의 먼쪽가지돌기에서의 포타슘 채널의 소단위인 Kv1.2를 가지돌기의 표면으로부터 내재화시킨다는 사실이 최근 알려진 바, 고유해마의 CA3 영역의 추체세포에서의 내재적 흥분성의 장기강화가 먼쪽가지돌기로 들어오는 관통가지입력 및 중간가지돌기로 들어오는 연접/맞교차입력에서의 시냅스를 통한 입력의 변조에 영향을 미칠 수 있는지에 대한 의문이 제기되었다.

본 실험은 고유해마의 CA3 영역에서 수행되었다. 관통가지-추체세포 시냅스 및 연접/맞교차-추체세포 시냅스에서의 흥분성 후시냅스 전위를 전류고정법을 통해 8초 간격으로 관찰한 후, 신경세포체에의 역치전류 이상의 전류주입을 통해 2초간 10 Hz 빈도의 활동전압을 유발시켰다. 이후 같은 방법으로 흥분성 후시냅스 전위를 계속적으로 관찰한 결과, 10 Hz 빈도의 활동전압은 관통가지-추체세포 연접에서의 흥분성 후시냅스 전위만을 강화시키며 흥분성 후시냅스 전류는 강화시키지 않았다. 연접/맞교차-추체세포 시냅스에서는 흥분성 후시냅스 전류와, 흥분성 후시냅스 전위 모두 유의하게 변하지 않았다.

고유해마 CA3 영역에서의 관통가지-추체세포 시냅스의 내재적 흥분성의 장기강화와 metaplsticity의 관계를 규명하기 위해, 관통가지-추체세포 시냅스에서 시냅스앞 자극만으로 장기강화를 유발할 수 있는 관통가지 자극의 강도를 결정하였다. 여기에서, 최소강도 자극으로 관통가지-추체세포 시냅스를 자극하였을 때는 그 자체로서는 시냅스의 장기강화를 일으킬 수 없음을 확인하였다. 이를 약한 강도의 고빈도 자극이라 부르겠다. 약한 강도의 고빈도 자극에 있어서는 흥분성 후시냅스 전위와 활동전위의 연결 및 장기강화의 유도 그 어느 것도 일어나지 않았으나 신경세포체에의 전류주입을 통한 10 Hz 빈도의 활동전압 발생을 통해 내재적 흥분성을 장기강화했을 때는 약한 강도의 고빈도자극을 통해서도 흥분성 후시냅스 전위와 활동전위가 연결되고 관통가지-추체세포 시냅스의 장기강화가 유도됨이 확인되었다.

본 실험에서, 고유해마 CA3 영역의 추체세포에서의 내재적 흥분성의 장기강화는 흥분성 후시냅스 전위와 활동전압의 연결 가능성을 관통가지에서 특이적으로 증강한다는 사실을 규명할 수 있었다. 이것은 본 시냅스에서 Hebb의 법칙에 의거하여 기억의 형성에 기여하게 될 것이라고 생각되는 바이다.

중심단어: 해마, 장기강화, 내재적 가소성, metaplasticity

학번: 2012-21801